Anat Embryol (1991) 184:195–212

Anatomy and Embryology

Development and migration of Purkinje cells in the mouse cerebellar primordium *

Shigeki Yuasa[1], **Koki Kawamura**[1], **Katsuhiko Ono**[2], **Tohru Yamakuni**[3], **and Yasuo Takahashi**[4]

[1] Department of Anatomy, School of Medicine, Keio University, Tokyo 160, Japan
[2] Third Department of Anatomy, Okayama University Medical School, Okayama 700, Japan
[3] Department of Neuroscience, Mitsubishi-Kasei Institute of Life Sciences, Tokyo 194, Japan
[4] Department of Neuropharmacology, Brain Research Institute, Niigata University, Niigata 951, Japan

Accepted March 7, 1991

Summary. The mode of Purkinje cell migration in the mouse cerebellar primordium was examined immunohistochemically, by marking Purkinje cells with anti-spot 35 antibody and labeling them with 5′-bromodeoxyuridine. The cells migrated radially from the neuroepithelium of the fourth ventricle towards the cortical surface between the 13th and 17th days (E13–E17) of gestation. Regional differences in the migratory process were evident: the final settlement of the Purkinje cells proceeded earlier in the lateral and posterior parts of the primordium, exhibiting latero-medial and posteroventral-anterodorsal diminishing sequences. To elucidate the factors involved in the migration, the arrangement of radial glial fibers, and expression of the cell adhesion molecule, tenascin, were examined immunohistochemically with the monoclonal antibody 1D11, a marker for both immature and mature astroglia, and an anti-tenascin antibody. At E14, 1D11-immunopositive fibers were seen to extend from the ventricle to the pial surface, and the cell bodies of immature glia migrated after E15 towards the cortex, shortening the radial processes whose end-feet were attached to the pia mater. Tenascin, which possesses a neuron-glial adhesiveness, was also expressed on the radial fibers during the migration of the Purkinje cells. The fibers were closely apposed to the migratory Purkinje cells, and their arrangement and orientation accorded with the migratory direction of the Purkinje cells. Further, changes in the molecular species of antigens detected by both the 1D11 and anti-tenascin antibodies were observed by immunoblotting analysis during the course of cerebellar development. These findings suggest that the arrangement of radial glia and expression of adhesion molecules may be involved in the control and guidance of Purkinje cell migration.

Key words: Cerebellum – Purkinje cells – Migration – Radial fibers – Contact guidance

* This paper is dedicated to Professor Fred Walberg on the occasion of his 70th birthday

Offprint requests to: K. Kawamura

Introduction

In the development of the central nervous system, neuroblasts are generated from the neuroepithelium of the ventricles (the ventricular zone of the Boulder Committee 1970), and they migrate towards destined positions after the final mitosis. The migratory cells are guided by contact with radial glial fibers in the cerebral cortex (Rakic 1985; Gadisseux et al. 1990), the hippocampus (Nowakowski and Rakic 1979; Rickmann et al. 1987) and the cerebellar cortex (Rakic 1985). Neuroblasts differentiate, extend processes and form neural circuits through the processes of specific recognition and synaptogenesis. In the mouse cerebellum, precursors of Purkinje cells complete the final mitosis at embryonic days 11 to 13 (E11–E13), as demonstrated previously in a ^{3}H-thymidine autoradiographic study (Miale and Sidman 1961). The mode of migration of the embryonic Purkinje cells, and factors which control and define the detailed processes are little understood despite several studies of rodents (Wassef and Sotelo 1984; Altman and Bayer 1985a, b; Morris et al. 1985).

Spot 35 protein is expressed specifically in Purkinje cells in the cerebellum, and this protein can be detected from the embryonic stages (Takahashi-Iwanaga et al. 1986). On the other hand, 5′-bromodeoxyuridine (BrdU) is incorporated into the nuclear DNA of mitotic cells as a thymidine analogue, and those cells which have integrated BrdU into the chromosomal DNA can be detected immunohistochemically with anti-BrdU antibody in the developing brain (Yoshida et al. 1987; Miller and Nowakowski 1988).

We investigated the process of migration of mouse Purkinje cells by marking them with both anti-spot 35 antibody and BrdU. Special attention was paid to temporal and regional differences. We further studied the radial structures in the migratory routes by using markers for immature glia, i.e., anti-vimentin antibody (Bovolenta et al. 1984) and monoclonal antibody 1D11 (Ono et al. 1989). We also undertook immunohistochemical examinations of the expression of the cell adhesion

molecule, tenascin (Erickson and Bourdon 1989), in the cerebellar primordium. Tenascin, which is also known as cytotactin (Grumet et al. 1985), J1 (Faissner et al. 1988) and hexabrachion (Erickson and Taylor 1987), is one of the substrate adhesion molecules which influence the processes of neuron-glia adhesion and cell migration at critical developmental stages of the nervous tissue (Crossin et al. 1990). In a recent study by Prieto et al. (1990), this molecule was shown to be synthesized in the developing chick cerebellum by radial glia, and is present along the glial fibers. Under these circumstances, we attempted to elucidate the correlative interaction between Purkinje cell migration and the substrate components.

Materials and methods

Animals

Inbred pregnant mice of the C3H/HeJ JcI strain were used. The day when vaginal plugs were first observed was taken as embryonic day 0 (E0) and the day of birth was taken as postnatal day 0 (P0).

Immunohistochemistry

Detection of cells which integrated 5'-bromodeoxyuridine. In pregnant mice at the 12th day of gestation (E12), 5'-bromodeoxyuridine (BrdU, Sigma) was administered intravenously three times daily (each dose, 80 mg/kg) at 6-h intervals (i.e., at 08:00, 14:00 and 20:00). Under Nembutal anesthesia, E13–E18 fetuses were dissected free from the uterine cavity. The heads of E13–E16 mice and whole brains of E17–E18 mice were immersion-fixed in 95% ethanol and 5% acetic acid at 4° C for 12 h. They were then dehydrated, embedded in paraffin and sectioned at 10 μm. The sections were deparaffinized and immersed in 0.1 M HCl for 15 min at 4° C to extract basic nucleoproteins, and to expose the nuclear DNA. After rinsing in 100 mM phosphate-buffered saline (PBS, pH 7.4), containing 0.85% NaCl, the sections were immersed in 1 mM phosphate buffer (PB, pH 7.4) containing 0.0085% NaCl and 50% formamide (Wako Pure Chemical, Osaka) at 80° C for 5 min to denature and unwind the double-helical DNA so as to expose BrdU to the anti-BrdU antibody. The sections were immediately transferred to ice-cold 80% ethanol to prevent the chromosomal DNA from annealing and renaturing. The denaturation temperature was lowered by 20° C with 50% formamide, which also maintained the quality of the tissue morphology. The tissue sections were then incubated with anti-BrdU antibody (Becton-Dickinson, 1:50 dilution) at 4° C overnight. After rinsing in PBS, the sections were incubated with horseradish peroxidase (HRP)-labeled Fab'-fragment of anti-mouse IgG (MBL, Nagoya) (1:40 dilution) at room temperature for 1 h. After rinsing again in PBS, the HRP reaction was performed in 0.02% diaminobenzidine (DAB, Dojindo Lab., Kumamoto) and 0.006% H_2O_2 in 50 mM Tris-HCl buffer (TB, pH 7.4).

Immunohistochemical detection of the expression of spot 35 protein. In some experiments, adjoining sections were subjected to BrdU- and spot 35-immunohistochemistry. In other experiments, the heads of E14–E15 embryos were dissected free and fixed by immersion in 4% paraformaldehyde in 0.1 M PB (pH 7.4) for 48 h at 4° C. Transcardiac perfusion was performed in E16–E18 mice with 20 ml of 4% paraformaldehyde, and the brains were further immersion-fixed in the same fixatives for 48 h at 4° C. Following fixation, the brains were immersed in 20% sucrose in 0.1 M PB, frozen on crushed dry ice, and sections were cut with a cryostat (Reichert-Jung). The paraffin sections for BrdU immunohistochemistry or cryostat sections were incubated with anti-spot 35 antibody (Yamakuni et al. 1984) (1:1000 dilution) at 4° C overnight. After rinsing in PBS, the sections were incubated with HRP-labeled Fab'-fragment of anti-rabbit IgG (MBL, Nagoya) (1:40 dilution) at room temperature for 1 h. After rinsing again in PBS, the HRP reaction was performed in DAB-H_2O_2 solution.

Immunohistochemical detection of vimentin. The heads of mouse embryos (E14–E17) were fixed by immersion in a mixture of formalin-acetic acid-80% ethanol (5:5:90) at 4° C for 5 h. After washing with 80% ethanol, the material was dehydrated and embedded in paraffin. Sections were then immunostained with anti-vimentin antibody (ICN ImmunoBiologicals, Ill., USA) (1:50 dilution) as the primary antibody and HRP-labeled Fab'-fragment of anti-goat IgG (MBL, Nagoya) (1:40 dilution) as the secondary antibody.

Immunohistochemical detection of tenascin and neurofilament (160 kD). The heads of E14–E16 mice and brains of E17–E18 mice were fixed with 4% paraformaldehyde in 0.1 M PB (as in the spot 35 immunohistochemistry). Cryostat sections were immunostained with anti-tenascin antibody (Chemicon, Calif., USA) (1:1000 dilution) as the primary antibody and HRP-labeled Fab'-fragment of anti-rabbit IgG as the secondary antibody or with anti-neurofilament (160 kD) antibody (Amersham, UK) (1:50 dilution) as the primary antibody and HRP-labeled Fab'-fragment of anti-mouse IgG as the secondary antibody.

Immunohistochemistry of monoclonal antibody 1D11. Cryostat sections of paraformaldehyde-fixed E14–E18 brains (see the above spot 35 and tenascin immunohistochemistry) were also immunostained with monoclonal antibody 1D11 (1:1 dilution) (Ono et al. 1989) as the primary antibody and HRP-labeled Fab'-fragment of anti-mouse IgG as the secondary antibody. Most sections adjacent to those treated immunohistochemically were stained with cresyl violet.

Sodium dodecyl sulfate-polyacrylamide gel electrophoresis (SDS-PAGE) and immunoblotting of proteins in the developing mouse cerebellum

Mouse cerebella at E14–E16 and P20 were dissected free and homogenized in ten volumes of lysis buffer (4% SDS, 9 M urea and 5% mercaptoethanol in 0.0625 M Tris-HCl buffer, pH 6.8). The homogenates were syringed through a 23-gauge needle to shear the DNA and to lower the viscosity of the homogenate. The resultant samples were electrophoresed on a 7% gel according to the method of Laemmli (1970). After the electrophoresis, the separated proteins were transferred onto a nitrocellulose membrane filter BA85SD (0.45 μm in pore size, Schleicher & Schuell, Dassel) following the procedure of Towbin et al. (1979). The blotted membrane was incubated with 5% skimmed milk in 20 mM Tris-HCl buffer containing 2.9% NaCl (pH 7.5, Tris-buffered saline, TBS) to block non-specific binding, and each lane was incubated separately at 4° C overnight with the following primary antibodies: anti-tenascin, monoclonal 1D11 or anti-vimentin antibodies. After rinsing in TBS, each strip was incubated with HRP-labeled secondary antibody at room temperature for 1 h, employing HRP-labeled Fab'-fragment of anti-rabbit IgG for anti-tenascin antibody, HRP-labeled Fab'-fragment of anti-mouse IgG for monoclonal antibody 1D11, and HRP-labeled Fab'-fragment of anti-goat IgG for anti-vimentin antibody, respectively. The HRP reaction was then carried out by incubation with DAB/H_2O_2 solution.

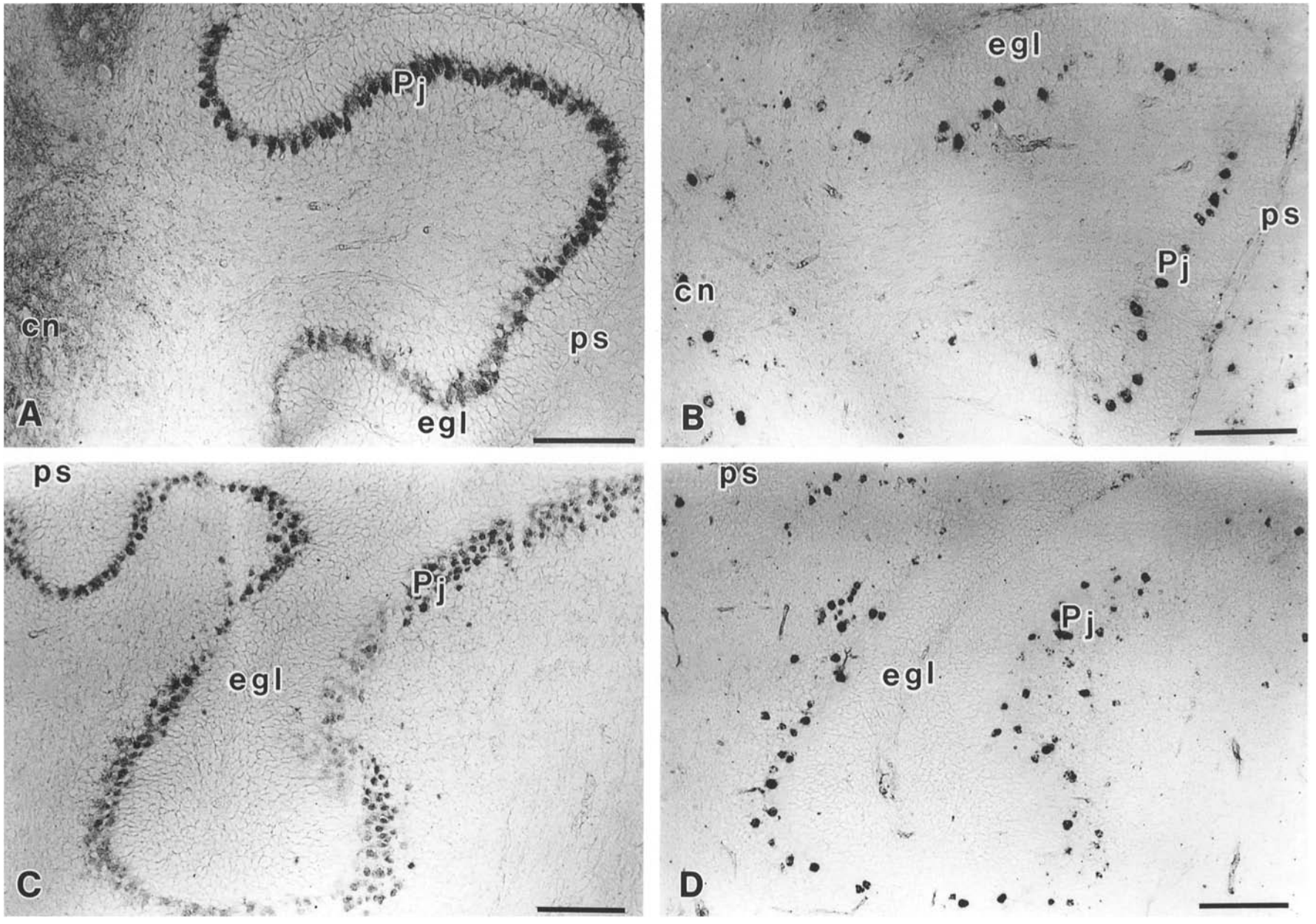

Fig. 1 A–D. Photomicrographs of parasagittal (**A** and **B**) and coronal (**C** and **D**) sections of the P2 mouse cerebellum, immunostained with anti-spot 35 (**A** and **C**) or anti-BrdU (**B** and **D**) antibodies. BrdU was administered intravenously to pregnant mice at the 12th day of gestation. The immunopositive cells are localized in the Purkinje cell layer and in the cerebellar nuclear region. Scale bars 100 μm. Abbreviations and orientations in this and subsequent figures are as follows: *cb*, cerebellum; *cn*, cerebellar nuclei; *egl*, external granular layer; *imz*, intermediate zone; *m*, medulla oblongata; *Pj*, Purkinje cell (layer); *ps*, pial surface; *svz*, subventricular zone; *V4*, fourth ventricle. In all photomicrographs of the cerebellum, top is dorsal and bottom is ventral. Also, left is rostral and right is caudal in parasagittal sections; left is medial and right is lateral in coronal sections

Results

Identification of cerebellar cells labeled with BrdU at E12

BrdU was administered to pregnant mice at E12 and the offspring were sacrificed at P2. Immunohistochemical staining of the materials obtained was carried out with anti-BrdU and anti-spot 35 antibodies. At P2, BrdU-labeled cells were arranged discontinuously in one or two layers (Fig. 1B, D) and their distribution was identical to that of cells immunoreactive to anti-spot 35 antibody (Fig. 1A, C) which specifically stains Purkinje cells in the cerebellar cortex (Yamakuni et al. 1984). Only a few cells in the cerebellar nucleus were labeled with BrdU (Fig. 1B).

Migratory patterns of cells labeled with BrdU at E12

The migratory process of mitotic cells, labeled with BrdU at E12, was observed in parasagittal sections of E13–E17 mice. At E13, most of the labeled cells appeared to be stratified in the subventricular zone. In the intermediate zone, we found migratory cells, most of which were probably precursors of Purkinje cells. Several cells reached the primordial cortical region only in the caudal half (Fig. 2A). The number of migratory labeled cells in the caudal primordial area was increased at E14 (Fig. 2B). At E15, rising numbers of labeled cells were seen approaching the cortex in the caudal part of the cerebellar primordium. In the rostro-dorsal part, however, only some of the cells reached the cortical region (Fig. 2C). Extensive areas of the cortex were covered with labeled cells at E16, while many other cells were still migrating from the subventricular to the intermediate zone (Fig. 2D). At E17, the majority of the labeled cells reached the cortex and formed stratified cell layers, although the number of labeled cells in the rostro-dorsal part of the cortex was apparently smaller, and migratory cells remained in the subcortical area (Fig. 2E).

It is of interest to note that Purkinje cells move through the cerebellar nuclei at E17 (Fig. 2E), while the Purkinje cells at E15 move around the nuclear cells which are also in the migratory stage (Fig. 2C; cf. E18 of rats (Altman and Bayer 1985b)).

Some cells, presumably granule cell precursors, were also labeled in the external granule cell layer of the E13–E15 primordia, since no labeled cells were found in the layer after E16: further division of the labeled cells may result in a dilution of the incorporated BrdU (Fig. 2).

Expression of spot 35 protein observed in parasagittal sections

Spot 35-immunopositive cells, corresponding to Purkinje cell precursors, were observed in the subventricular and intermediate zones of the E14 cerebellum. Most of the cells were found in the caudal half of the primordium, and few reached the cortex (Fig. 3A). At E15, the number of migratory cells was increased in the intermediate and cortical zones of the caudal part (Fig. 3B). Purkinje cells accumulated in the cortex at E16 (Fig. 3C). At E17, most of them were observed in the cortex, forming several rows of cell layers, except in the rostro-dorsal region, towards which many Purkinje cells were still migrating (Fig. 3D). In the entire cortex of the E18 cerebellum, it was clearly demonstrated that groups of Purkinje cells were arranged discontinuously in several layers, interrupted by groups of immunonegative cells (Fig. 3E).

Regional differences in the migration of spot 35-immunopositive cells observed in coronal sections

A medio-lateral difference was also evident in the process of migration of spot 35-immunopositive cells (considered as equal to Purkinje cells), as seen in coronal sections. In the entire E14 cerebellum, most of the spot 35-immunopositive cells were distributed homogeneously in both the subventricular and intermediate zones (Fig. 4A). In the lateral part of the E15 cerebellum, immunopositive cells accumulated in the intermediate zone (Fig. 4B). In the lateral part of the E16 primordium, many Purkinje cells had reached the cortex. In the medial part, however, the migration of Purkinje cells was retarded, and many of them still remained within the subventricular zone in the most medial portion (Fig. 4C). Across the entire E17 primordium, Purkinje cells were arranged in several layers and the cells were distributed from the intermediate zone to the cortex. In the lateral part, several discrete masses of Purkinje cells were formed, while in the medial part, the development of Purkinje cell layers was retarded (Fig. 4D). Small groups of spot 35-negative cells interrupted the continuous arrangement of spot 35-positive cell layers, as clearly observed in the E18 material (Fig. 5).

Morphological features of migratory Purkinje cells

From E14, spot 35-immunoreactive cells appeared in the cerebellar primordium (Figs. 3A and 6C), where the initial differentiation steps of immature Purkinje cells occurred. Different types of Purkinje cells were recognized: one type represented a round form with no apparent polarity, and was situated mainly in the subventricular zone; and the other type represented an elongated form with polarized processes correlated with the migratory direction (Fig. 6C). The latter possessed leading and/or trailing processes, which were arranged in the direction of the apparent migratory stream. The migratory cells of the elongated type were distributed mainly in the intermediate zone. The leading processes of the Purkinje cells changed their direction, from perpendicular to parallel relative to the pial surface, in the upper part of the intermediate zone of the E14–E15 cerebellum (Fig. 7B). As observed in adjoining sections stained with antineurofilament (160 kD) antibody, this region appeared to coincide with the trajectory area of afferent

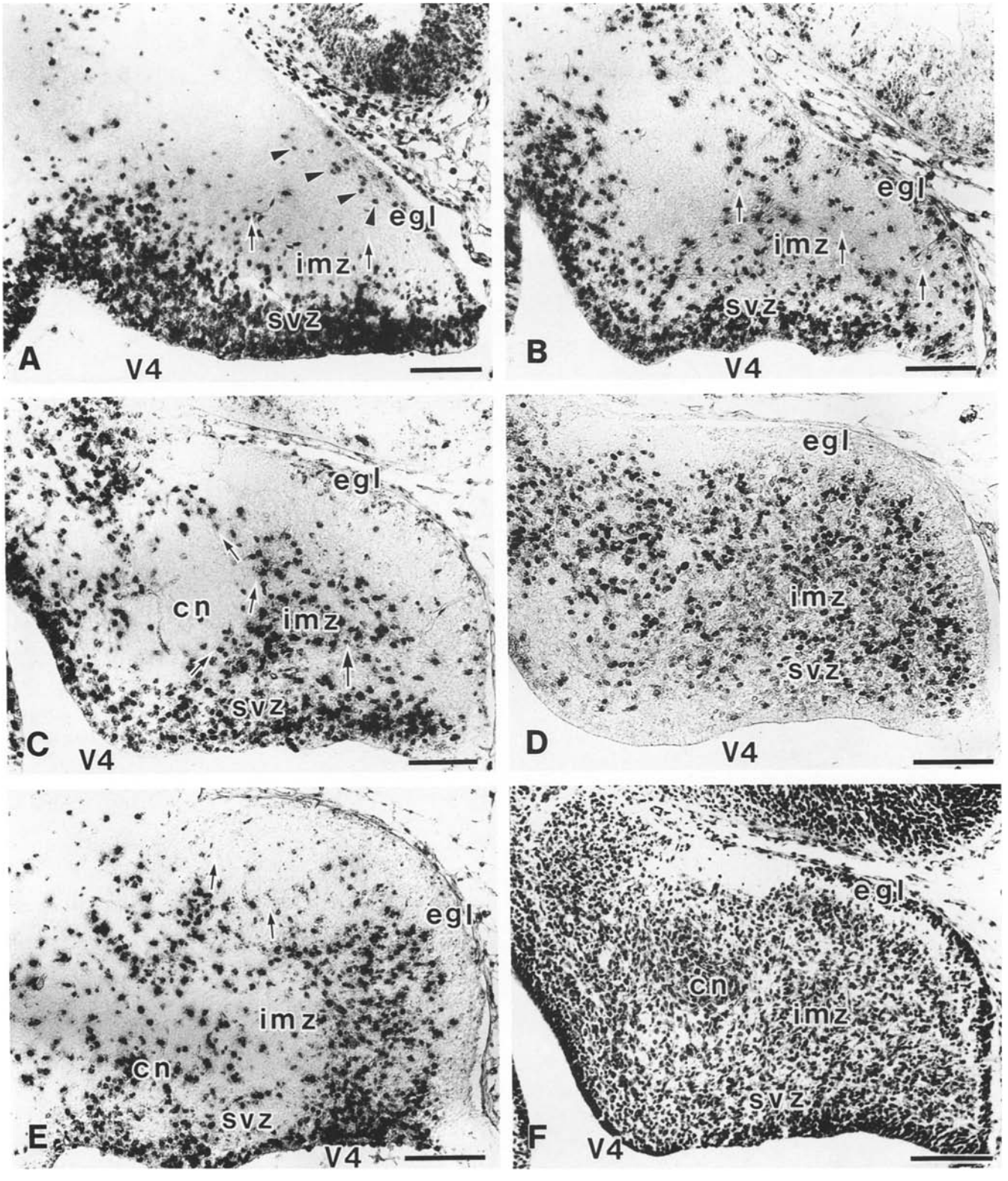

Fig. 2A–F. Photomicrographs of parasagittal sections of the mouse cerebellar primordium (E13–E17) showing the migratory patterns of BrdU-labeled cells. Pregnant mice at the 12th day of gestation were given BrdU, and sections from the fetal brains were immunostained with anti-BrdU antibody. Directions of migration are indicated by *arrows*. Scale bars 100 μm **A** (E13) Most of the labeled cells are in the subventricular zone. Many migratory cells are present in the intermediate zone and there are several cells (*arrowheads*) in the caudal half of the cortical primordium. **B** (E14) Many labeled cells are migrating in the intermediate zone towards the cortex, mainly in the caudal half of the primordium. **C** (E15) The number of labeled cells near the cortex is increased in the caudal half of the primordium. In the rostro-dorsal region, labeled cells are migrating around a presumed nuclear region. **D** (E16) The entire cortex is largely covered with labeled cells, and many others are still migrating in the intermediate zone. **E** (E17) Labeled cells form stratified cell layers in the caudal part of the cortex. In the rostro-dorsal part, however, the number of labeled cells is much smaller, and migratory cells remain in the subcortical area. Regional differences in development are apparent. **F** Photomicrograph showing the presence of cells in the nuclear region of the E15 cerebellum. Nissl-stained section adjacent to **C**

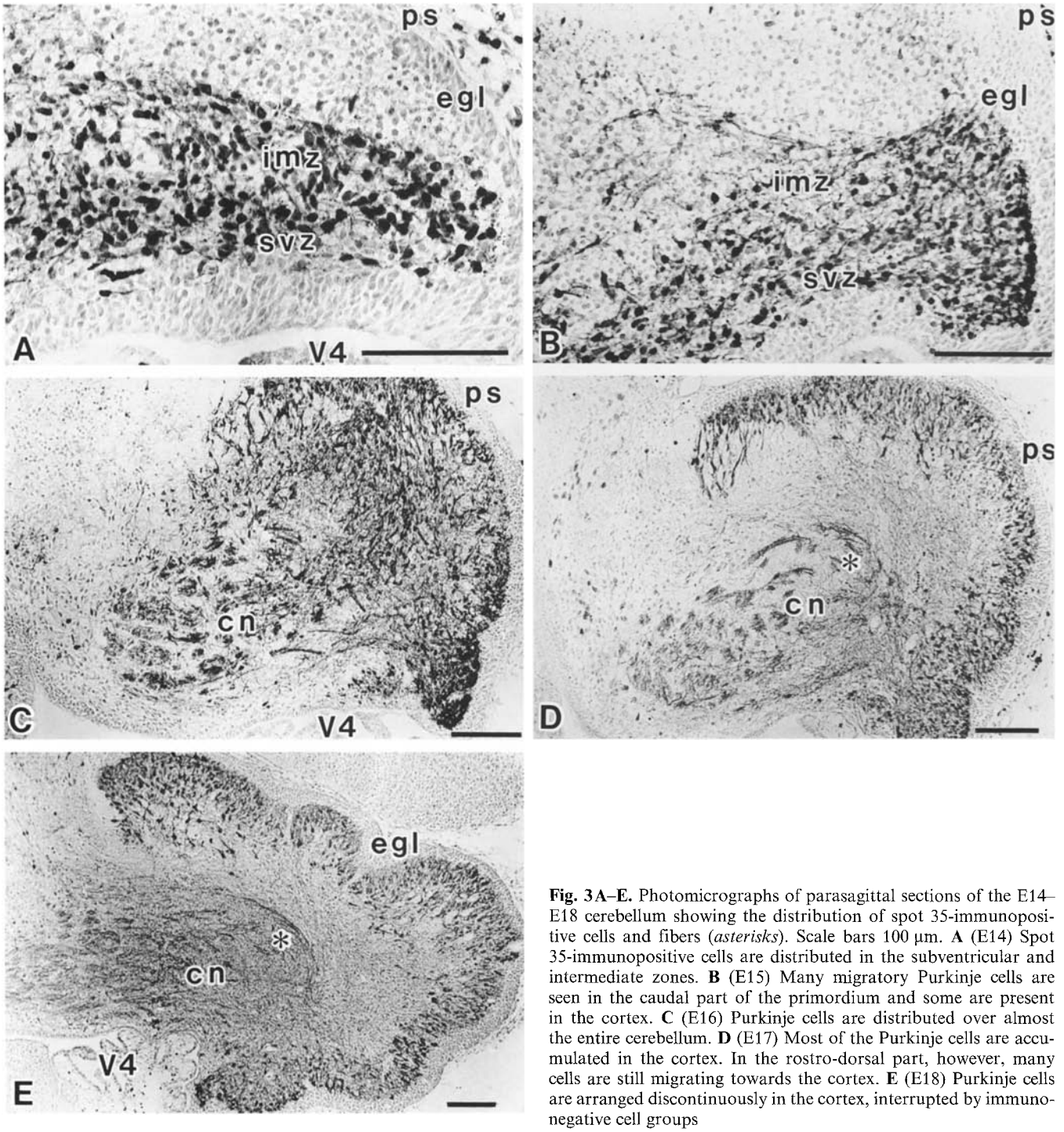

Fig. 3A–E. Photomicrographs of parasagittal sections of the E14–E18 cerebellum showing the distribution of spot 35-immunopositive cells and fibers (*asterisks*). Scale bars 100 μm. **A** (E14) Spot 35-immunopositive cells are distributed in the subventricular and intermediate zones. **B** (E15) Many migratory Purkinje cells are seen in the caudal part of the primordium and some are present in the cortex. **C** (E16) Purkinje cells are distributed over almost the entire cerebellum. **D** (E17) Most of the Purkinje cells are accumulated in the cortex. In the rostro-dorsal part, however, many cells are still migrating towards the cortex. **E** (E18) Purkinje cells are arranged discontinuously in the cortex, interrupted by immunonegative cell groups

fibers from the dorsal part of the medulla oblongata, presumably from the vestibular nuclei (Fig. 7A). Thus, the change in direction of the migratory Purkinje cells in this area may be caused by the route of growing vestibulo-cerebellar fiber bundles.

At E17–E18, formation of cortex by the migratory cells was delayed in the rostro-dorsal area as compared to other regions (Fig. 3D, E). In this delayed area, typical spot 35-immunoreactive cells bearing leading and/or trailing processes were found (Fig. 8C). In addition, in parasagittal (Fig. 3D, E) and coronal (Fig. 4D) sections after E17, spot 35-immunoreactive fibers were seen to enter the region of the cerebellar nuclei, apparently extending from migratory Purkinje cells as well as from those already settled in the cortex.

Immunohistochemical observation of vimentin-immunopositive structures

Employing an immature astroglia marker (Bovolenta et al. 1984), examinations were made of vimentin-immu-

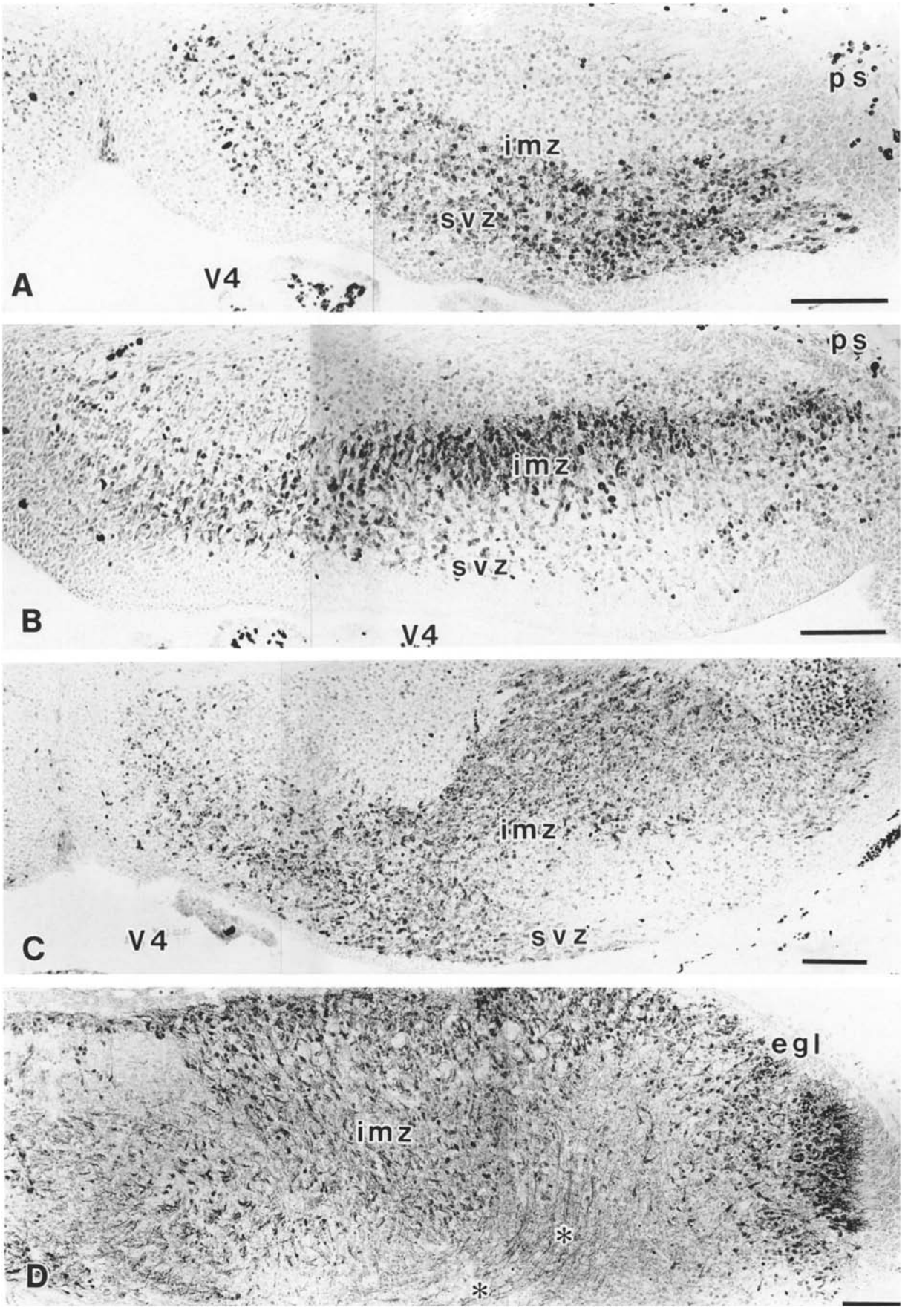

Fig. 4A–D. Photomicrographs of coronal sections of the E14–E17 cerebellum showing regional differences in the migration of spot 35-immunopositive cells. Scale bars 100 μm. **A** (E14) Most of the Purkinje cells are distributed in the subventricular and intermediate zones. **B** (E15) Many Purkinje cells accumulate in the intermediate zone of the lateral part. **C** (E16) In the lateral part of the primordium, many Purkinje cells are seen in the cortex, but their migration is retarded in the medial portion. **D** (E17) Over the entire cortex, the Purkinje cells are arranged to form layers with several rows. Particularly in the lateral part of the cortex, several masses of Purkinje cells are formed. Immunopositive fibers are indicated by *asterisks*

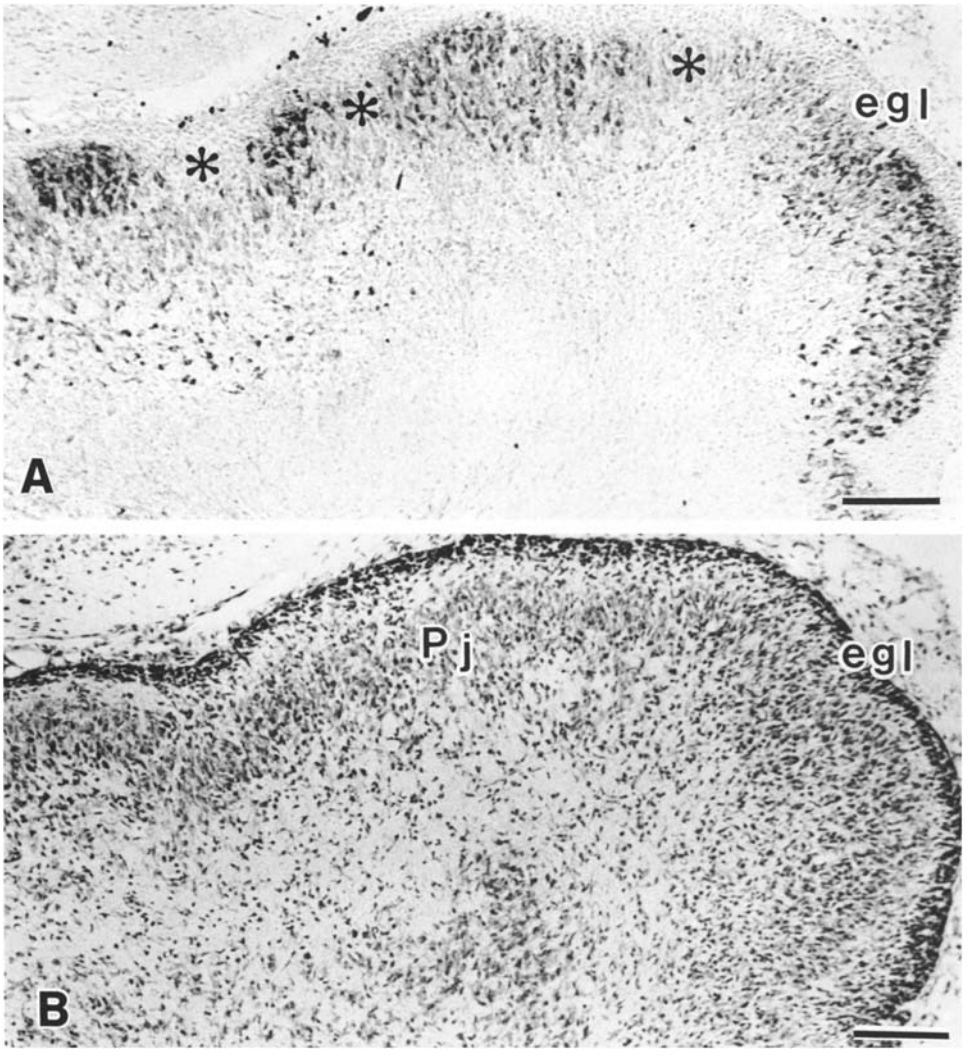

Fig. 5A, B. Photomicrographs of coronal sections of the E18 cerebellum. Scale bars 100 μm. **A** Several rows of spot 35-immunopositive cells occur discontinuously in the cortex, interrupted by immunonegative cell groups (*asterisks*). **B** An adjacent section to Fig. 5A stained with cresyl violet. Note that several rows of Purkinje cells are arranged continuously in the cortex

noreactive structures in the cerebellar primordium. From E14, vimentin immunoreactivity was apparent in radial fibers which extended from the surface of the fourth ventricle (Fig. 9B) to the pial surface (Fig. 9A). Vimentin-immunoreactive cell bodies were observed in the ventricular zone. By Nomarsky optics, a close apposition of elongated or round cells to the vimentin-positive fibers was clear. In the subventricular and intermediate zones, the direction of the fibers and the arrangement of the apposed cells coincided with the migratory stream of Purkinje cells (Fig. 9A, B). The fibers in the ventricular and subventricular zones remained recognizable until E17 (Fig. 10B).

Observation of monoclonal antibody 1D11-immunoreactive structures

From E14, 1D11-immunoreactive structures were observed in the cerebellar primordium. Radial fibers immunoreactive to 1D11 extended from the ventricular zone to the subpial region (Fig. 6A). 1D11-immunoreactive cell bodies were also noted in the ventricular zone (Fig. 6A, B). The direction of these fibers coincided with the migratory stream of the Purkinje cells. The structures were found to be denser and more distinct in the medial part than in the lateral part of the E14 cerebellum. At E15 (Fig. 10A), 1D11-immunoreactive cell bodies were identified in the subventricular zone, and they apparently migrated towards the cortex, with the radial fibers arranged in the direction of movement. Expression of 1D11 antigen in the membrane of the glial cell bodies was also observed (Fig. 10A'). Some of the 1D11-immunoreactive cell bodies exhibited an elongated form. Spot 35-immunoreactive cells and 1D11-immunoreactive cell bodies were intermingled in the subventricular zone, and 1D11-immunoreactive cell bodies also underwent migration, following the Purkinje cells which had started to migrate earlier. By E17, 1D11-immunoreactive cell bodies reached the caudo-dorsal part of the cortex, at which most of the Purkinje cells had already arrived (Fig. 8B). The 1D11-immunoreactive processes had become shortened, with their end-feet attached to the pia mater. The 1D11-immunoreactive structures resembled in appearance the Bergmann glia of the postnatal cerebellum. In the rostro-dorsal region of the E17–E18 cortical primor-

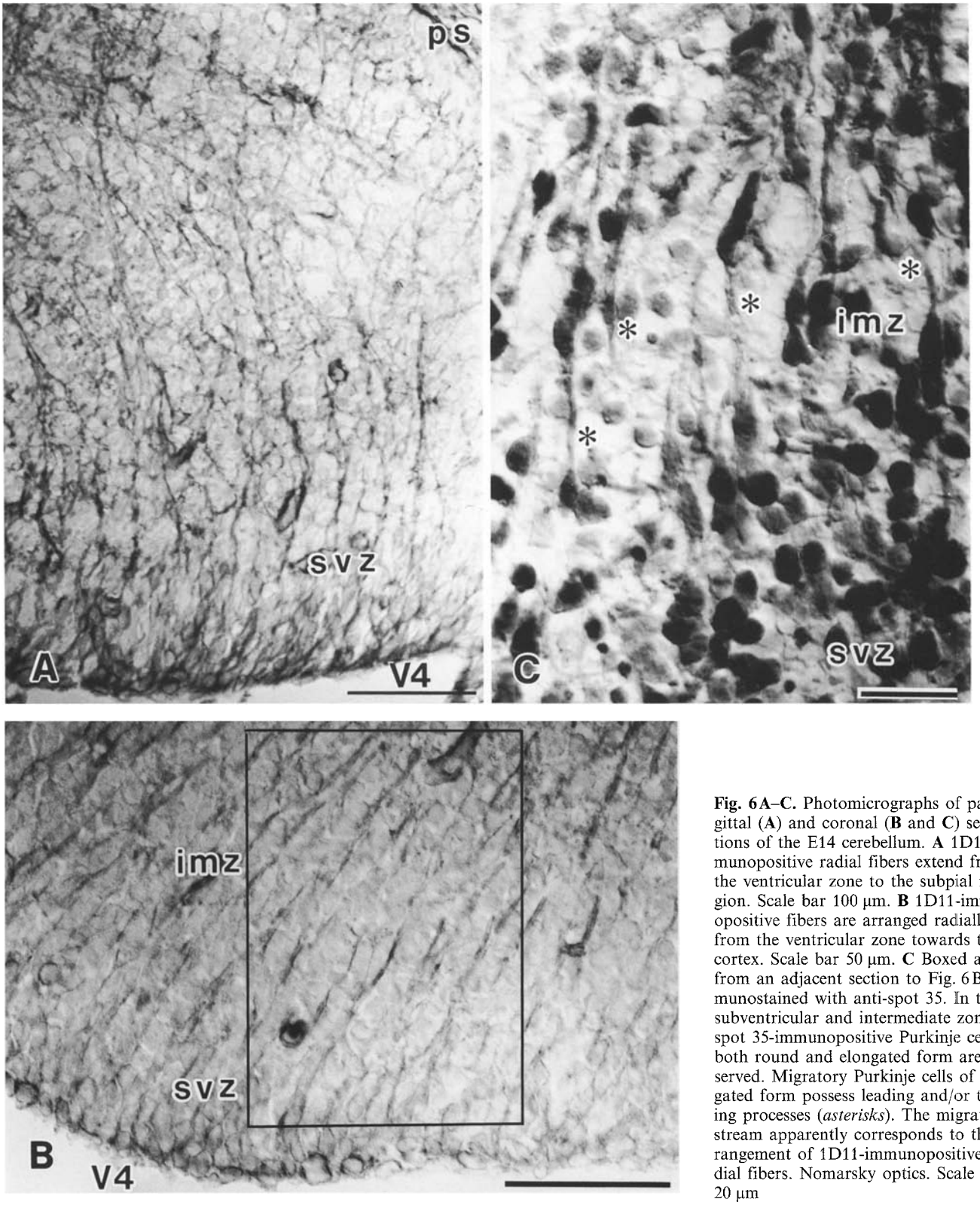

Fig. 6A–C. Photomicrographs of parasagittal (**A**) and coronal (**B** and **C**) sections of the E14 cerebellum. **A** 1D11-immunopositive radial fibers extend from the ventricular zone to the subpial region. Scale bar 100 μm. **B** 1D11-immunopositive fibers are arranged radially from the ventricular zone towards the cortex. Scale bar 50 μm. **C** Boxed area from an adjacent section to Fig. 6B, immunostained with anti-spot 35. In the subventricular and intermediate zones, spot 35-immunopositive Purkinje cells of both round and elongated form are observed. Migratory Purkinje cells of elongated form possess leading and/or trailing processes (*asterisks*). The migratory stream apparently corresponds to the arrangement of 1D11-immunopositive radial fibers. Nomarsky optics. Scale bar 20 μm

dium (Fig. 8A), where the arrival and layer formation of Purkinje cells were relatively delayed as compared to other regions, migratory Purkinje cells were still present (Fig. 8C), and 1D11-immunoreactive radial fibers remained distinct (Fig. 8A) despite the shortening of the radial fibers in other parts of the cortex.

Tenascin-immunoreactive structure in the cerebellar primordium

Tenascin is a cell adhesion molecule which is believed to mediate the interaction between neurons and glia in developing nervous tissues (Erickson and Bourdon

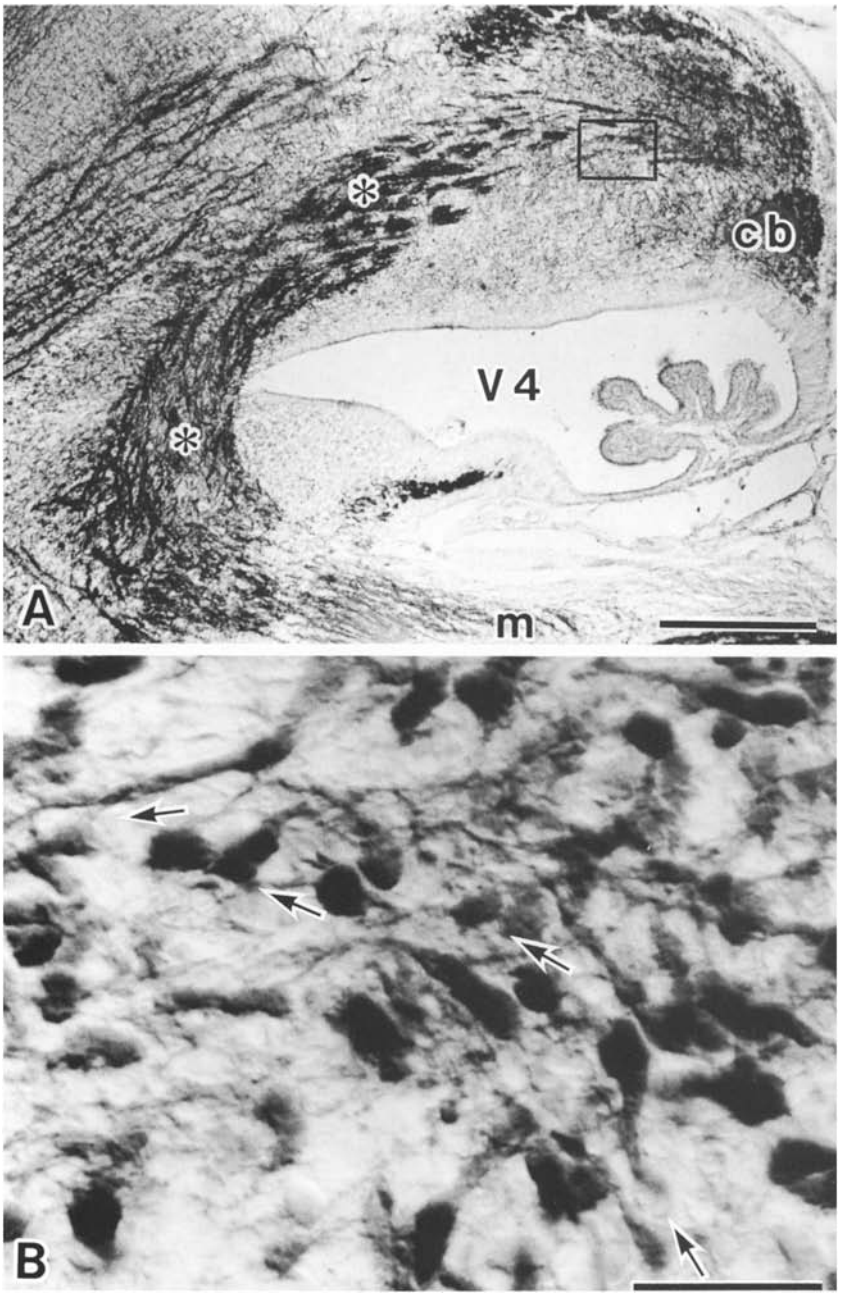

Fig. 7A, B. Photomicrographs of parasagittal sections of the E14–E15 cerebellum. **A** Afferent fibers, immunostained with anti-neurofilament (160 kD) antibody (*asterisks*), entering the intermediate zone of the cerebellum from the dorsal part of the primordial medulla. Scale bar 200 μm. **B** Spot 35-immunopositive Purkinje cells changing their migratory direction (*arrows*) from perpendicular to parallel relative to the pial surface in the intermediate zone, as observed in the boxed area of an adjacent section to **A**. Nomarsky optics. Scale bar 20 μm

1989). This molecule is synthesized by the glia and is considered to be identical or closely related to the J1-molecule (Kruse et al. 1985), cytotactin (Hoffman et al. 1988) and hexabrachion (Erickson and Taylor 1987). At E14, tenascin-immunoreactive radial fibers were found to extend from the ventricular zone to the pia mater (Fig. 11A–C). These radial fibers were likewise arranged in the direction of Purkinje cell migration. The density of the fibers was higher in the medial half of the primordium where Purkinje cells were migrating massively towards the cortex, than in the lateral half where many Purkinje cells were already approaching the cortex (not shown in the figures). After E17, the expression of tenascin immunoreactivity in the radial fibers was noted in the cortical part of the primordium with a diminished intensity. Weak immunoreactivity was observed over the cerebellar tissue in both the cell structures and extracellular space.

Apposition of migratory Purkinje cells to radial fibers observed in horizontal sections of the cerebellar primordium

Serial horizontal sections of the E14–E15 cerebellar primordium were immunostained by antibodies of anti-spot 35 (Fig. 12A), anti-tenascin (Fig. 12B) and 1D11 (Fig. 12C). Spot 35-immunopositive migratory cells were apparently apposed to the radial fibers with 1D11 or tenascin immunoreactivity. Complexes of migratory cells and tenascin- or 1D11-immunoreactive radial fibers

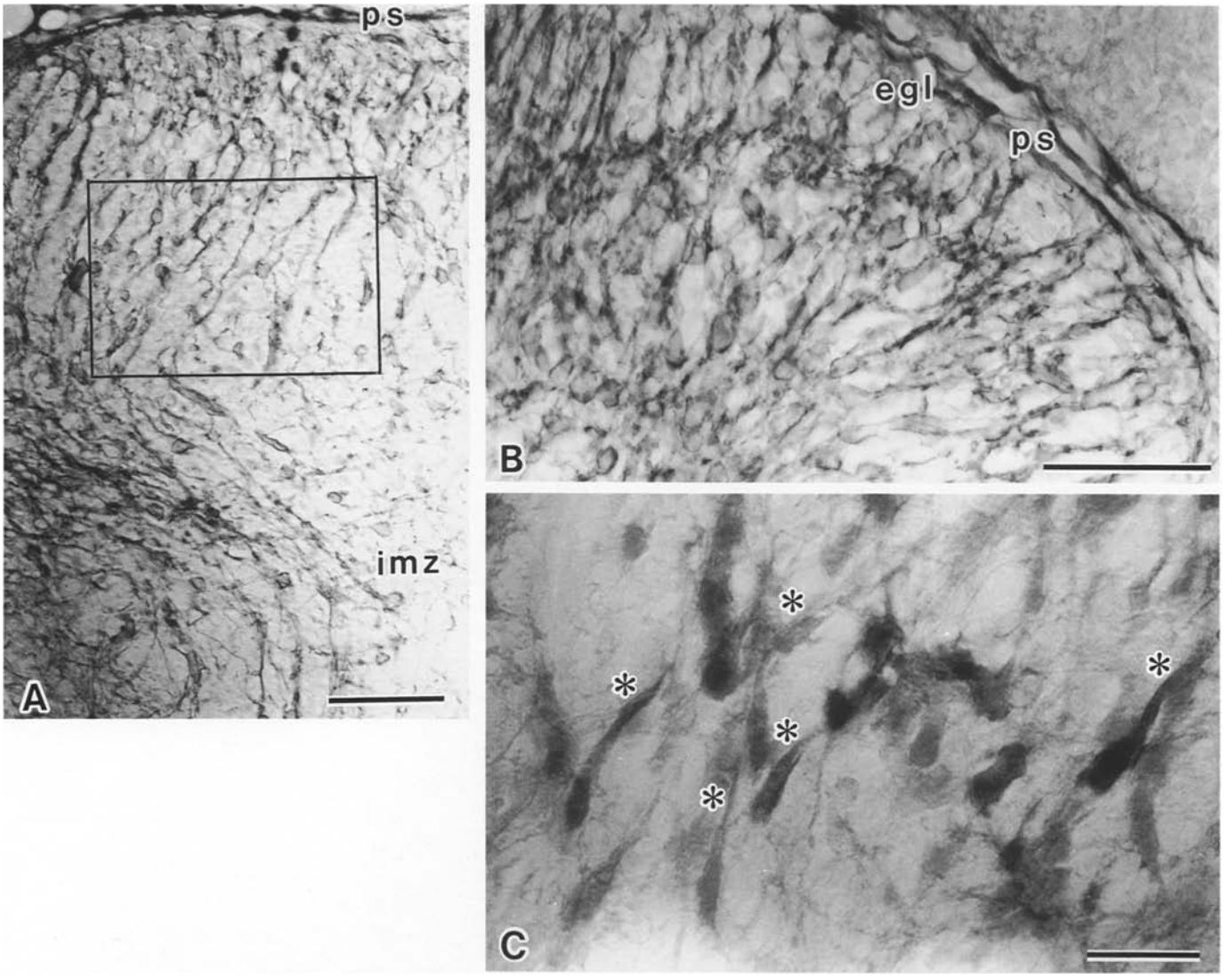

Fig. 8A–C. Photomicrographs of parasagittal sections of the E17 cerebellum. **A** 1D11-immunopositive radial fibers still extend from the intermediate zone to the subpial region in the rostro-dorsal region. Scale bar 50 μm. **B** 1D11-immunopositive cell bodies are distributed in the caudo-dorsal portion of the cortex with processes extending into the subpial region. Scale bar 50 μm. **C** Many spot 35-immunopositive cells bearing leading processes (*asterisks*) are still migrating in the rostro-dorsal region, as observed in the boxed area of an adjacent section to **A**. The direction of their arrangement corresponds to that of the 1D11-immunopositive radial fibers in **A**. Scale bar 20 μm

were therefore plotted diagrammatically (Fig. 12A′, B′, C′). The distribution pattern of each immunoreactive fiber attached to spot 35-immunoreactive cells was found to be similar. The diameters of the 1D11-immunoreactive radial fibers (Fig. 12C), however, appeared to be larger than those of the tenascin-immunoreactive radial fibers (Fig. 12B). Usually one to several radial fibers were apposed to a presumed migrating cell. 1D11-immunoreactive cell bodies were occasionally observed among the fibers and migratory Purkinje cells (Fig. 12C).

Immunochemical analysis of marker proteins for the immature glial cell lineage

Electrophoresis of proteins in both embryonic and adult mouse cerebella was carried out using SDS-polyacrylamide gels (7%). They were then transferred to nitrocellulose filters and reacted with antibodies of 1D11, anti-tenascin or anti-vimentin. Vimentin protein was expressed as a single band corresponding to a molecular weight (MW) of 57 kD, and the apparent molecular weight was found to be constant during development from embryo to adult (Fig. 13C). In contrast, the antigens recognized by 1D11 monoclonal antibody underwent changes of molecular species (Fig. 13B). In the embryonic cerebellum (E15), a band corresponding to a MW of 110 kD was dominant. In the adult cerebellum, however, a band corresponding to a MW of 40 kD became dominant. The antigens recognized by anti-tenascin anti-body also changed their molecular weight during development (Fig. 13A). At E14, the antibody recognized bands corresponding to MW 205 kD and MW

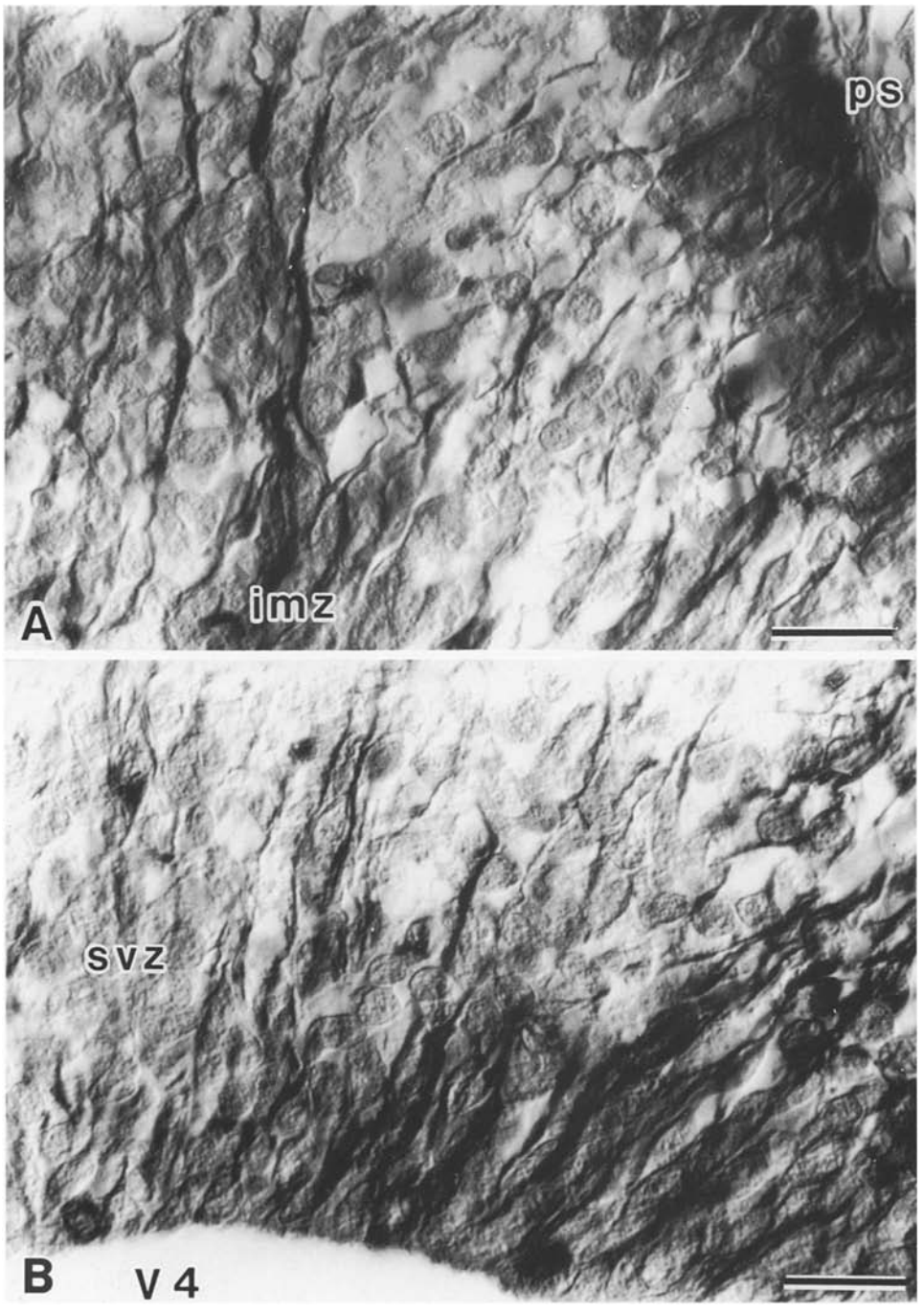

Fig. 9A, B. Photomicrographs of parasagittal sections of the E14 cerebellum immunostained with anti-vimentin antibody, in the intermediate zone and cortical region (**A**) and in the subventricular zone (**B**). Migratory cells are apparently apposed to immunopositive radial fibers. Nomarsky optics. Scale bars 20 μm

220 kD. At E15–E16, when the Purkinje cells underwent massive migration, the expression of these bands was increased. Later, however, the bands faded and the band corresponding to MW 205 kD disappeared from the adult cerebellum.

Discussion

In the present study, the initial expression of spot 35 immunoreactivity in the mouse cerebellar primordium was demonstrated at E14. On the other hand, spot 35-immunopositive cells have been observed in the rat embryonic cerebellum from E17 (Takahashi-Iwanaga et al. 1986). The birth date of mouse Purkinje cells is E11–E13 (Miale and Sidman 1961; Inouye and Murakami 1980), while that of rat Purkinje cells is E12–E15 (Altman and Bayer 1978). Here, the day of sperm positivity was considered as E0. The difference of 3 days in the initial expression of spot 35 immunoreactivity between mice and rats may well be related to the difference of 2 days in the birth date of the Purkinje cells between the two animals. Thus, the expression of spot 35 immunoreactivity is generally considered to be initiated several days after the final mitosis in rodent Purkinje cell precursors.

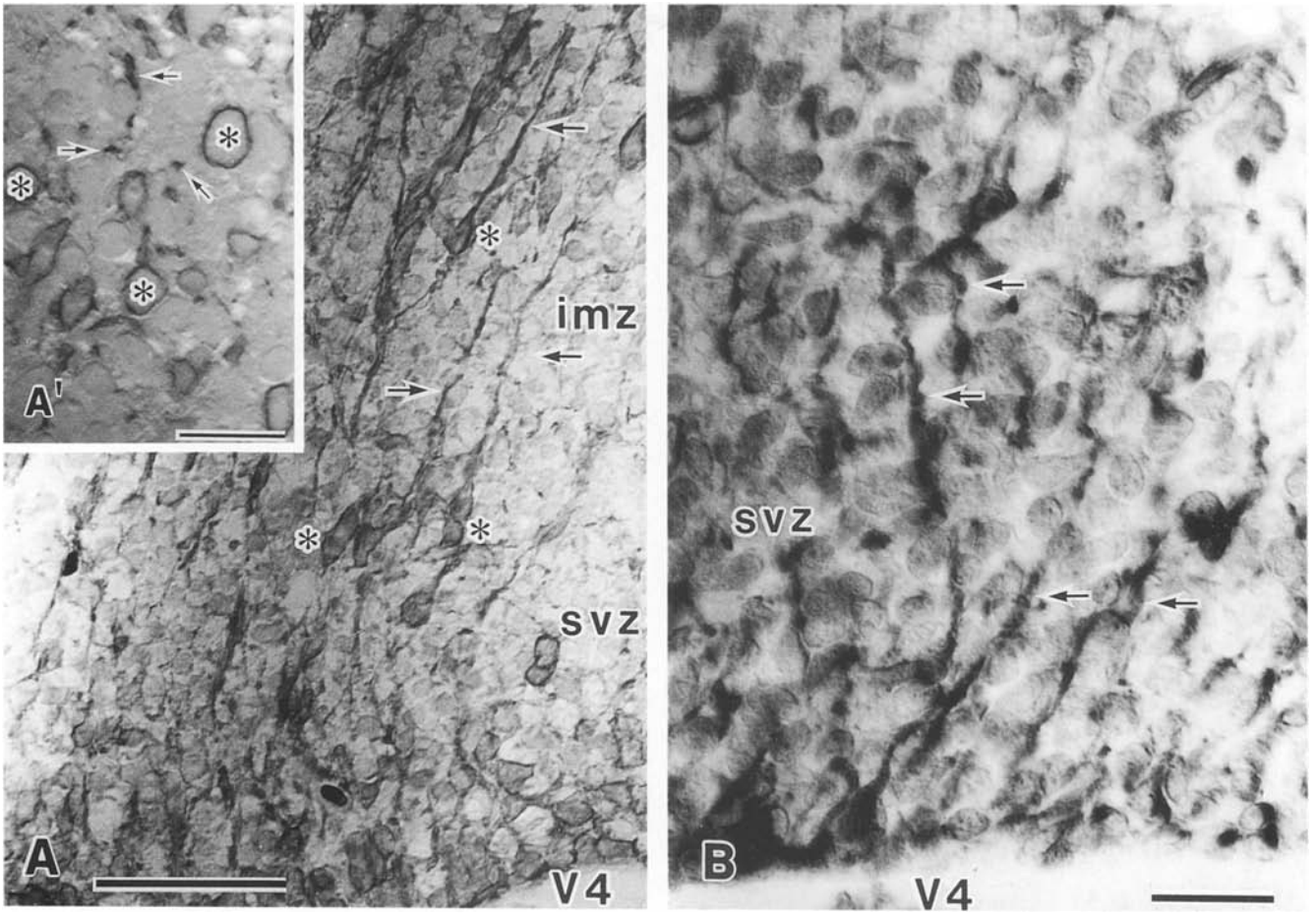

Fig. 10. **A** Photomicrograph of a coronal section of the E15 cerebellum immunostained with 1D11. Immunopositive cells (*asterisks*) are migrating from the subventricular zone towards the cortex, with the radial fibers (*arrows*) arranged in the direction of movement. Radial fibers are obviously decreased in the ventricular zone. Scale bar 50 μm. **A'** Photomicrograph of a horizontal section, cut through the subventricular zone, of the E15 cerebellum immunostained with 1D11. Note that the plasma membrane of the glial cell bodies (*asterisks*) and radial glial processes (*arrows*) were both immunopositive. Scale bar 20 μm. **B** Photomicrograph of a parasagittal section of the E17 cerebellum immunostained with anti-vimentin antibody. Immunopositive radial fibers (*arrows*) from the ventricular zone still remain. Nomarsky optics. Scale bar 20 μm

Several clusters of spot 35-immunopositive cells were formed in the Purkinje cell layer of the mouse cerebellar primordium (E18) (Fig. 5). In the rat perinatal cerebellum, transient heterogeneity in the expression of several Purkinje cell markers has also been reported (Wassef et al. 1985). When Purkinje cells were labeled with BrdU at E12 and examined at P2 in the present study, the labeled cells were found to be discontinuously arranged, partly forming groups (Fig. 1). In the chick embryonic cerebellum, Purkinje cells labeled with ^{3}H-thymidine at the final mitotic period also form longitudinal bands in the cortex (Kanemitsu and Kobayashi 1988). A recent study employing chimeric mice (Wetts and Herrup 1982) has indicated that the progenitors which are committed to differentiate into the entire population of cerebellar Purkinje cells constitute eight kinds in C3H/HeJ mice. Such multiplicity of progenitor cells can be reflected in a heterogeneous population of developing Purkinje cells.

Furthermore, a regional heterogeneity in the differentiation of Purkinje cells can be created by extrinsic factors such as developing cerebellar afferents or the chemical microenvironment of the extracellular matrices. The transient longitudinal organization of spot 35-immunopositive cells in the Purkinje cell layer is reminiscent of the parasagittal organization of the olivocerebellar projection observed in cats (Groenewegen and Voogd 1977; Kawamura and Hashikawa 1979; Brodal and Kawamura 1980) and rats (Chan-Palay et al. 1977). According to Mason et al. (1990), climbing fibers in mice have already reached the multilayered zone of Purkinje cells at birth. It has also been demonstrated that the parasagittal organization of the olivocerebellar topography is already established in the newborn rat (Sotelo et al. 1984). It is possible therefore that growing afferents may induce or maintain the zonal expression of spot 35 immunoreactivity in the continuously arranged Purkinje cells in the cortex, as observed in the E18 mouse cerebellum (Fig. 5). Cortico-nuclear fibers also exhibit a parasagittal organization pattern (Dietrichs and Walberg 1979, 1980; Voogd and Bigare 1980; Dietrichs 1981a, b, 1983). After E16 in mice, presumed axons of Purkinje cells reach the nuclear region (Figs. 3C–E, and 4D). Early

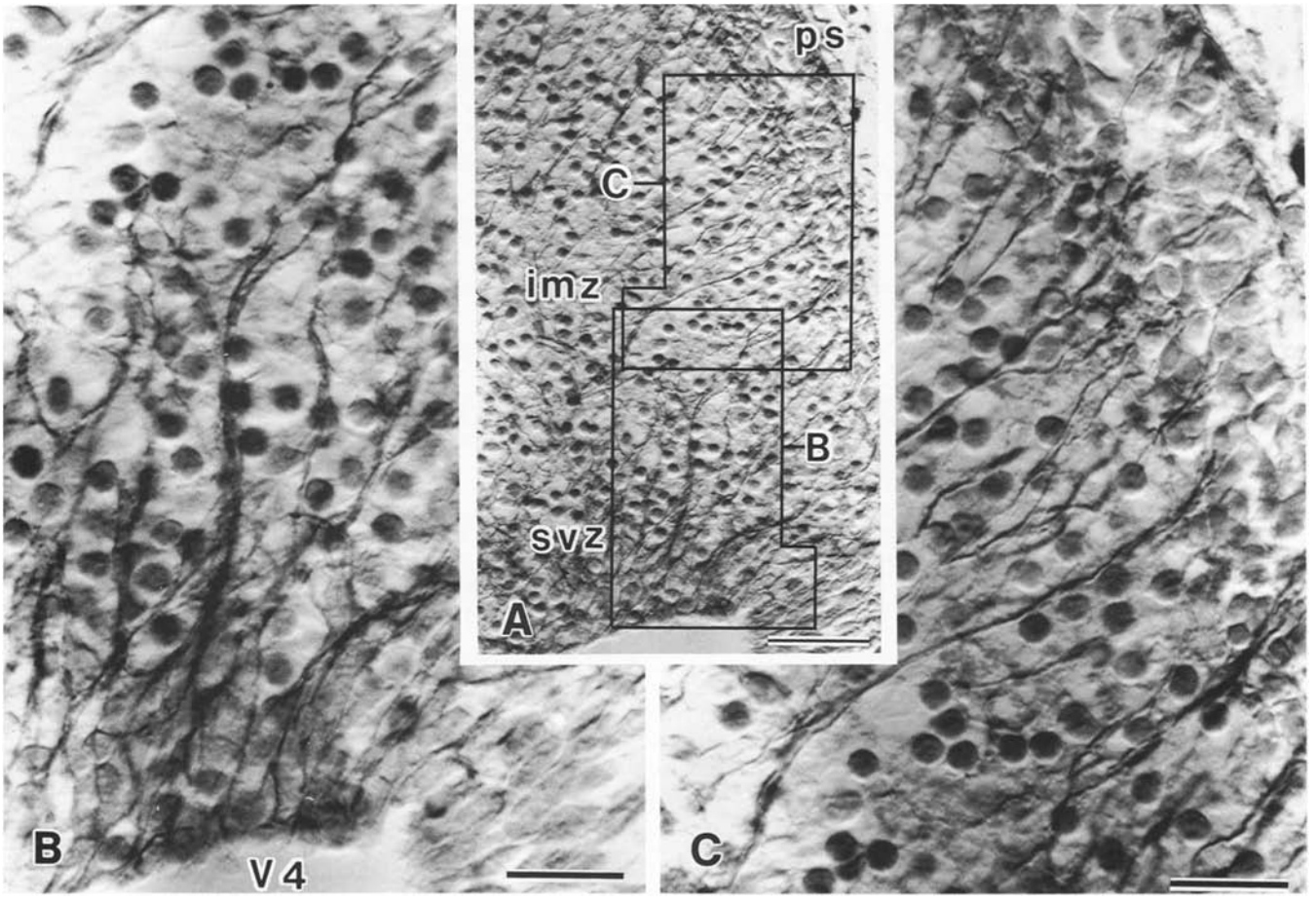

Fig. 11A–C. Photomicrographs of parasagittal sections of the E14 cerebellum immunostained with anti-tenascin antibody. Radial fibers extend from the ventricular zone to the cortex (**A**), parts of which are magnified in **B** and **C**. Nomarsky optics. Scale bar 50 μm in **A**, and 20 μm in **B** and **C**

contact between immature Purkinje and nuclear cells might be responsible for the maintenance of expression of the spot 35 immunoreactivity in a zonal pattern at the late embryonic stages.

On the other hand, various factors are involved in the determination of the patterns of neuronal migration and settlement. These factors can be broadly grouped into two categories: one concerns regional and temporal differences in the intrinsic nature of the populations of neuronal precursors, while the other concerns the cellular and extracellular components which interact with migratory cells during development. A temporal gradient from the ventro-caudal to the dorso-rostral regions was revealed in the patterns of migration and settling of Purkinje cells, as demonstrated by the distribution and migration of BrdU-labeled cells and spot 35-immunopositive cells in the mouse embryonic cerebellum (Figs. 2 and 3). Such a caudo-rostral gradient in the regional differences of migratory pattern of Purkinje cells has also been observed in the rat cerebellar primordium by labeling the cells with ^{3}H-thymidine (Altman and Bayer 1985a, c). Furthermore, a latero-medial gradient in the migratory pattern was clearly demonstrated in the present study by means of the specific marker, spot 35, for Purkinje cells (Fig. 4).

Regional differences of mouse Purkinje precursors were not recognized in the E13 neuroepithelium when the BrdU incorporation was examined following administration at E12 (Fig. 2A). At E14–E15, however, differentiation of the neuroepithelial cells to spot 35-immunoreactive cells occurred earlier in the lateral and caudal than in the medial and rostral regions (Figs. 3A, B and 4A, B). As demonstrated also by Inouye and Murakami (1980), the final mitotic division occurs earlier for the Purkinje cells localized at the lateral level. It can be conjectured that an inherent heterogeneity of Purkinje cell precursors in the neuroepithelium may determine the regional differences in migratory pattern and final settlement of Purkinje cells.

In the present materials from E17–E18 brains, the rostral region of the cerebellar cortex was not yet occupied by settled Purkinje cells, and migratory cells were observed moving towards the area (Fig. 3D, E). These migratory Purkinje cells appeared to deviate in their course around the cerebellar nuclei which had been formed earlier. Thus, even though their birth dates are the same as those of other Purkinje cells, their final settlement in the cortex tends to be delayed. In addition, the trajectory of afferent fibers from the medulla oblongata to the intermediate zone of the cerebellar primor-

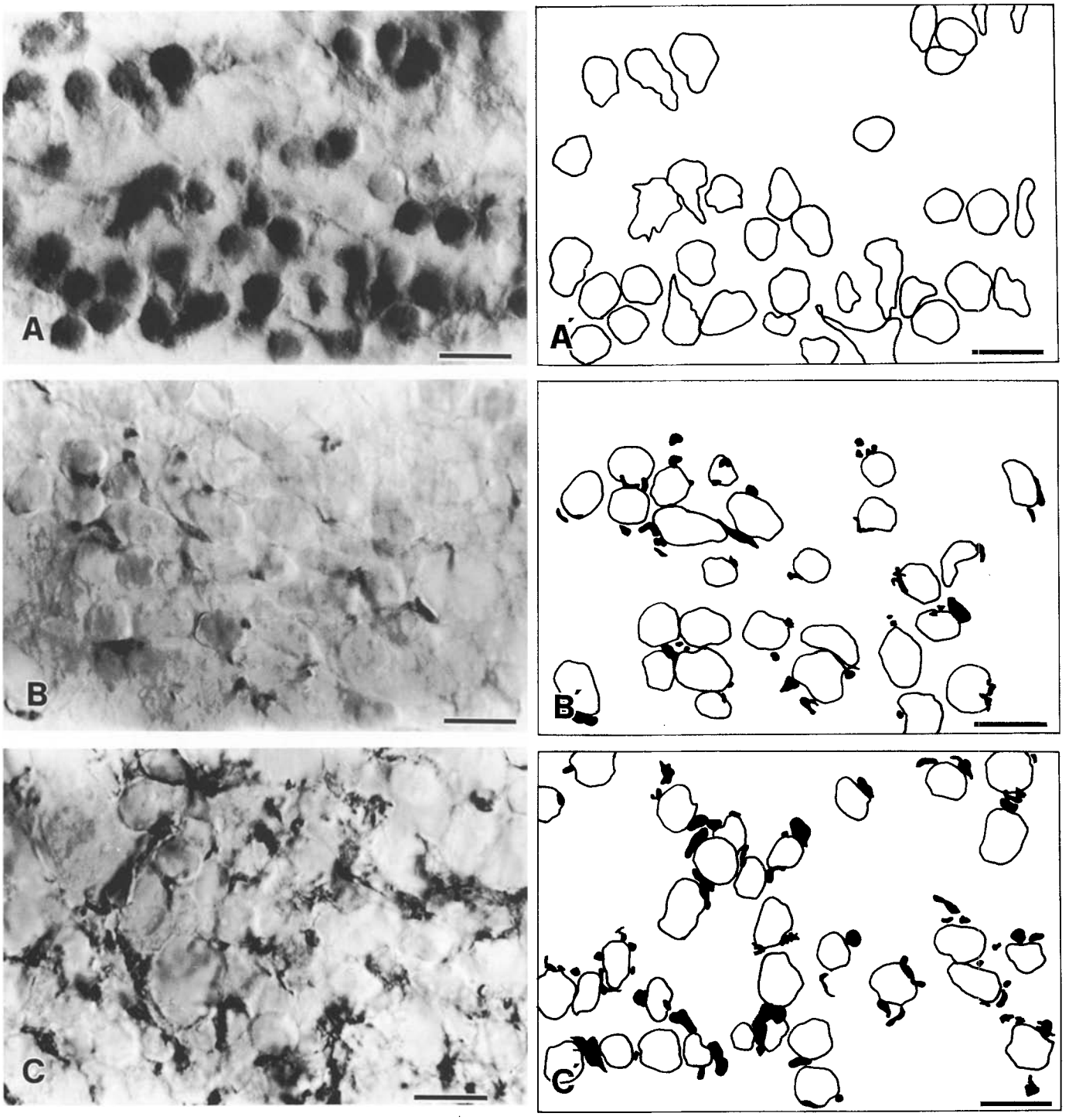

Fig. 12A–C. Photomicrographs (**A**, **B** and **C**) and diagrammatic drawings (**A′**, **B′** and **C′**) of sections of the E14–E15 cerebellum, cut horizontally at migratory zones, showing correlative locations between migratory Purkinje cells and radial fibers. Note that Purkinje cells, stained with anti-spot 35 antibody (**A** and **A′**), are closely apposed to the tenascin-immunopositive (**B** and **B′**) and 1D11-immunopositive (**C** and **C′**) radial fibers. The locations, sizes and shapes of the immunonegative, large cells in **B** and **C** equally correspond to spot 35-immunopositive Purkinje cells in **A**. Nomarsky optics. Scale bars 10 μm

dium may be responsible for change in the migratory course at E14–E15 (Fig. 7). These fibers are considered to be vestibulo-cerebellar fibers, which are the earliest cerebellar afferents, and reach mainly the caudal part of the cerebellar primordial cortex, so forming the anlage of the vestibulocerebellum (Morris et al. 1988).

The glial or matrix cells (Fujita 1963) and the extracellular matrices in the cerebellar primordium should also be regarded as important factors which are involved in the migration of Purkinje cells. Since Sidman and Rakic (1973) advocated the concept of contact guidance as an underlying mechanism in the migration of neuro-

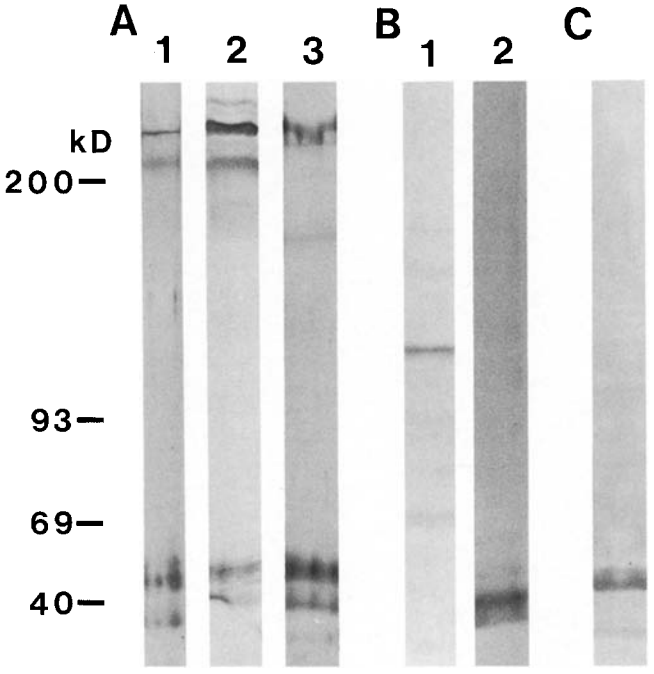

Fig. 13A–C. Immunoblotting analysis of tenascin and marker proteins for the glial cell lineage in the cerebellum. **A** Immunoblots stained with anti-tenascin antibody. *1*, E14; *2*, E16; *3*, adult. **B** Immunoblots stained with 1D11. *1*, E15; *2*, adult. **C** Immunoblot of the E14 cerebellum stained with anti-vimentin antibody

blasts in the developing brain, the correlations between neuroblast migration and the structural distribution of radial glia have been investigated, e.g., in the murine cerebral cortex (Gadisseux et al. 1989, 1990), monkey hippocampus (Nowakowski and Rakic 1979) and monkey cerebellum (Rakic 1985). Several authors (Del Cerro and Swarz 1976; Swarz and Oster-Granite 1978) have referred to the structural appearance of radial glia in the rodent embryonic cerebellum, but did not unambiguously show a relationship to and participation in the migration of Purkinje cells.

Expression of an antigen recognized by monoclonal antibody 1D11 has been observed as a marker for prenatal and postnatal astroglia in the cerebellum (Ono et al. 1989). In the present study, radial fibers with 1D11 immunoreactivity were found to extend from the ventricular zone to the pial surface during the E14–E17 period (Figs. 6 and 8). The dynamic transformation of the 1D11-immunoreactive radial fibers and their relation to migratory Purkinje cells were multiphasic. At first radial fibers extended from the ventricular zone to the pia mater at E14–E15 (Fig. 6A, B) and the arrangement of fibers was in accordance with the migratory stream of immature Purkinje cells (Fig. 12A, C). Then, as immature glia migrated from the ventricular zone, their processes retracted towards the cortex after E15 (Figs. 8A, B and 10A). Finally in the rostro-dorsal portion of the E17–E18 cerebellum, migration of Purkinje cells proceeded among radially arranged 1D11-immunoreactive fibers (Fig. 8A, C), and in other parts where Purkinje cell migration had almost finished, 1D11-immunoreactive radial fibers became transformed into presumptive Bergmann glia (Fig. 8B).

At E15, a large part of the Purkinje cells had started migration and some had reached the cortex. There is thus a few days' lag between the onset of Purkinje cell migration and the migration of the 1D11-immunopositive soma. In 2–3 days, the Purkinje cells and 1D11-immunopositive soma become aligned in the same layer of the cortex (Fig. 8B). The migration of the 1D11-immunoreactive cells and the shortening of their processes may therefore be triggered by contact interaction between the migrating Purkinje cells and 1D11-positive radial fibers. Neuronal influences on glial morphological changes and gene expression have been reported (Hatten 1985, 1990; Mason et al. 1988).

The molecular species reactive to 1D11 undergo changes in molecular weight during embryonic development (Fig. 13B). At around E15, when large numbers of Purkinje cells were migrating, a band with a molecular weight of 110 kD was expressed. During the course of development, this band disappeared, and a new band of 40 kD appeared. In the early stages (e.g. E15), 1D11 immunoreactivity was confined to the cellular components (radial fibers and cell bodies) (Figs. 6A, B and 10A, A′), but as development proceeded (after E17), the immunoreactivity extended to the extracellular spaces of the developing molecular layer of the cortex (Ono et al. 1989). The conversion of molecular species of the 1D11-antigen may thus be related to Purkinje cell migration at the early stages, and subsequently to granule cell migration at the later stages of cerebellar development.

The vimentin-immunopositve radial glial fibers were similar in their distribution pattern and structure to the 1D11-immunopositive ones (Figs. 6 and 9). After the 1D11-immunopositive elements (fibers and cell bodies) had migrated towards the cortex, the radial fibers immunoreactive to 1D11 became shortened (from E15) and those in the subventricular zone disappeared (Fig. 10A). In contrast, the vimentin-immunopositive fibers in this area remained recognizable until E16–E17 (Fig. 10B). It is unclear whether the immature radial glia of vimentin-immunopositive cells and those of 1D11-immunopositive cells are identical, with a common cell lineage. It could be that, at the transitional state of differentiation of the primitive cells into radial glial cells, expression of the 1D11 gene(s) may be initiated, followed by migration of the glial cells towards their final positions in the cortex to mature as Bergmann glia. On the other hand, immature matrix cells (Fujita 1963) with vimentin immunoreactivity may remain in the ventricular zone as a reservoir of multipotential stem cells for the neuronal or glial cell lineage. Migration of Purkinje cells could proceed in contact with these radial fibers of different cell lineages.

After E14, tenascin immunoreactivity was detected in the cerebellar primordium (Figs. 11 and 12B). The expression in the radial fibers resembled in appearance that of the vimentin- and 1D11-immunoreactive structures (Figs. 6 and 8–12). The tenascin-immunopositive elements changed their appearance in a similar manner

to the 1D11-immunopositive elements. The distribution and direction of their arrangement coincided with the migratory stream of Purkinje cells (Figs. 11 and 12A, B).

When considering the mechanism of neuronal migration from the standpoint of contact guidance, it is necessary to assume adhesion of migratory cells to the processes of radial glia. A cell-binding domain has been identified on the protein structure of tenascin and cytotactin (Bourdon and Rouslahti 1989; Friedlander et al. 1988). Structural analysis of tenascin and cytotactin by cDNA cloning revealed domains homologous to fibronectin type III repeats (Pearson et al. 1988; Jones et al. 1988, 1989). Such domains are recognized by the cellular receptors, i.e., integrins, for attachment to the Arg-Gly-Asp (RGD) sequence of the substrate adhesion molecule (Bourdon and Rouslahti 1989). From the above evidence, it seems highly probable that tenascin expression on radial glial processes in the cerebellar primordium is involved in the adhesion of migratory Purkinje cells. The molecular species recognized by the anti-tenascin antibody also undergo changes of molecular weight as the development of the primordium proceeds (Fig. 13A). Moreover, the developmental changes of J1, an analogous molecule to tenascin which occurs in the mouse cerebellum (Kruse et al. 1985), are also similar to our results. Changes in the molecular species of tenascin are induced by different splicing mechanisms of a single gene (Jones et al. 1989). These changes may be related to differences in the local and temporal nature of the adhesiveness between migratory neurons and radial glial fibers in the developing cerebellum.

Acknowledgments. This study was supported in part by Grants-in-Aid for Scientific Research on Priority Areas (Molecular basis of neural connection) from the Ministry of Education, Science and Culture, Japan, and research grants from Keio University.

References

Altman J, Bayer SA (1978) Prenatal development of the cerebellar system in the rat. I. Cytogenesis and histogenesis of the deep nuclei and cortex of the cerebellum. J Comp Neurol 179:23–48

Altman J, Bayer SA (1985a) Embryonic development of the rat cerebellum. I. Delineation of the cerebellar primordium and early cell movements. J Comp Neurol 231:1–26

Altman J, Bayer SA (1985b) Embryonic development of the rat cerebellum. II. Translocation and regional distribution of the deep neurons. J Comp Neurol 231:27–41

Altman J, Bayer SA (1985c) Embryonic development of the rat cerebellum. III. Regional differences in the time of origin, migration, and settling of Purkinje cells. J Comp Neurol 231:42–65

Boulder Committee (1970) Embryonic vertebrate central nervous system: revised terminology. Anat Rec 166:257–262

Bourdon MA, Ruoslahti E (1989) Tenascin mediates cell attachment through an RGD-dependent receptor. J Cell Biol 108:1149–1155

Bovolenta P, Liem RKH, Mason CA (1984) Development of cerebellar astroglia: transition in form and cytoskeletal content. Dev Biol 102:248–259

Brodal A, Kawamura K (1980) Olivocerebellar projection: A review. Adv Anat Embryol Cell Biol 64:1–140

Chan-Palay V, Palay SL, Brown JT, Van Itallie C (1977) Sagittal organization of olivocerebellar and reticulocerebellar projections: autoradiographic studies with ^{35}S-methionine. Exp Brain Res 30:561–576

Crossin KL, Prieto AL, Hoffman S, Jones FS, Friedlander DR (1990) Expression of adhesion molecules and the establishment of boundaries during embryonic and neural development. Exp Neurol 109:6–18

Del Cerro MP, Swarz JR (1976) Prenatal development of Bergmann glial fibres in rodent cerebellum. J Neurocytol 5:669–676

Dietrichs E (1981a) The cerebellar corticonuclear and nucleocortical projections in the cat as studied with anterograde and retrograde transport of horseradish peroxidase. III. The anterior lobe. Anat Embryol 162:223–247

Dietrichs E (1981b) The cerebellar corticonuclear and nucleocortical projections in the cat as studied with anterograde and retrograde transport of horseradish peroxidase. IV. The paraflocculus. Exp Brain Res 44:235–242

Dietrichs E (1983) The cerebellar corticonuclear and nucleocortical projections in the cat as studied with anterograde and retrograde transport of horseradish peroxidase. V. The posterior lobe vermis and the flocculo-nodular lobe. Anat Embryol 167:449–462

Dietrichs E, Walberg F (1979) The cerebellar corticonuclear and nucleocortical projections in the cat as studied with anterograde and retrograde transport of horseradish peroxidase. I. The paramedian lobule. Anat Embryol 158:13–39

Dietrichs E, Walberg F (1980) The cerebellar corticonuclear and nucleocortical projections in the cat as studied with anterograde and retrograde transport of horseradish peroxidase. II. Lobulus simplex, Crus I and II. Anat Embryol 161:83–103

Erickson HP, Bourdon MA (1989) Tenascin: an extracellular matrix protein prominent in specialized embryonic tissues and tumors. Annu Rev Cell Biol 5:71–92

Erickson HP, Taylor HC (1987) Hexabrachion proteins in embryonic chicken tissues and human tumors. J Cell Biol 105:1387–1394

Faissner A, Kruse J, Chiquet-Ehrismann R, Mackie E (1988) The high-molecular-weight J1 glycoproteins are immunochemically related to tenascin. Differentiation 37:104–114

Friedlander DR, Hoffman S, Edelman GM (1988) Functional mapping of cytotactin: proteolytic fragments active in cell-substrate adhesion. J Cell Biol 107:2329–2340

Fujita S (1963) The matrix cell and cytogenesis in the developing central nervous system. J Comp Neurol 120:37–42

Gadisseux JF, Evrard P, Misson JP, Caviness VS (1989) Dynamic structure of the radial glial fiber system of the developing murine cerebral wall: an immunocytochemical analysis. Dev Brain Res 50:55–67

Gadisseux JF, Kadhim HJ, van den Bosch de Aguilar P, Caviness VS, Evrard P (1990) Neuron migration within the radial glial fiber system of the developing murine cerebrum: an electron microscopic autoradiographic analysis. Dev Brain Res 52:39–56

Groenewegen HJ, Voogd J (1977) The parasagittal zonation within the olivocerebellar projection. I. Climbing fiber distribution in the vermis of cat cerebellum. J Comp neurol 174:417–488

Grumet M, Hoffman S, Crossin KL, Edelman GM (1985) Cytotactin, an extracellular matrix protein of neural and non-neural tissues that mediates glia-neuron interaction. Proc Natl Acad Sci USA 82:8075–8079

Hatten ME (1985) Neuronal regulation of astroglial morphology and proliferation in vitro. J Cell Biol 100:384–396

Hatten ME (1990) Riding the glial monorail: a common mechanism for glial-guided neuronal migration in different regions of the developing mammalian brain. TINS 13:179–184

Hoffman S, Crossin KL, Edelman GM (1988) Molecular forms, binding functions, and developmental expression patterns of cytotactin and cytotactin-binding proteoglycan, an interactive pair of extracellular matrix molecules. J Cell Biol 106:519–532

Inouye M, Murakami U (1980) Temporal and spatial patterns of

Purkinje cell formation in the mouse cerebellum. J Comp Neurol 194:499–503

Jones FS, Burgoon MP, Hoffman S, Crossin KL, Cunningham BA, Edelman GM (1988) A cDNA clone for cytotactin contains sequences similar to epidermal growth factor-like repeats and segments of fibronectin and fibrinogen. Proc Natl Acad Sci USA 85:2186–2190

Jones FS, Hoffman S, Cunningham BA, Edelman GM (1989) A detailed structural model of cytotactin: protein homologies, alternative RNA splicing, and binding regions. Proc Natl Acad Sci USA 86:1905–1909

Kanemitsu A, Kobayashi Y (1988) Time of origin of Purkinje cells and neurons of the deep cerebellar nuclei of the chick embryo examined by ^{3}H-thymidine autoradiography. Anat Anz 165:167–175

Kawamura K, Hashikawa T (1979) Olivocerebellar projections in the cat studied by means of anterograde axonal transport of labeled amino acids as tracers. Neuroscience 4:1615–1633

Kruse J, Keilhauer G, Faissner A, Timpl R, Schachner M (1985) The J1 glycoprotein: a novel nervous system cell adhesion molecule of the L2/HNK-1 family. Nature 316:146–148

Laemmli UK (1970) Cleavage of structural proteins during the assembly of the head of bacteriophage T4. Nature 227:680–685

Mason CA, Edmondson JC, Hatten ME (1988) The extending astroglial process: development of glial cell shape, the growing tip, and interactions with neurons. J Neurosci 8:3124–3134

Mason CA, Christakos S, Catalano SM (1990) Early climbing fiber interactions with Purkinje cells in the postnatal mouse cerebellum. J Comp Neurol 297:77–90

Miale IL, Sidman RL (1961) An autoradiographic analysis of histogenesis in the mouse cerebellum. Exp Neurol 4:277–296

Miller MW, Nowakowski RS (1988) Use of bromodeoxyuridine-immunohistochemistry to examine the proliferation, migration and time of origin of cells in the central nervous system. Brain Res 457:44–52

Morris RJ, Beech JN, Barber PC, Raisman G (1985) Early stages of Purkinje cell maturation demonstrated by Thy-1 immunohistochemistry on postnatal rat cerebellum. J Neurocytol 14:427–452

Morris RJ, Beech JN, Heizmann CW (1988) Two distinct phases and mechanisms of axonal growth shown by primary vestibular fibres in the brain, demonstrated by parvalbumin immunohistochemistry. Neuroscience 27:571–596

Nowakowski RS, Rakic P (1979) The mode of migration of neurons to the hippocampus: a Golgi and electron microscopic analysis in foetal rhesus monkey. J Neurocytol 8:697–718

Ono K, Yanagihara M, Mizukawa K, Yuasa S, Kawamura K (1989) Monoclonal antibody that binds to both the prenatal and postnatal astroglia in rodent cerebellum. Dev Brain Res 50:154–159

Pearson CA, Pearson D, Shibahara S, Hofsteenge J, Chiquet-Ehrismann R (1988) Tenascin: cDNA cloning and induction by TGF-beta. EMBO J 7:2677–2981

Prieto AL, Jones FS, Cunningham BA, Crossin KL, Edelman GM (1990) Localization during development of alternatively spliced forms of cytotactin mRNA by in situ hybridization. J Cell Biol 111:685–698

Rakic P (1985) Mechanisms of neuronal migration in developing cerebellar cortex. In: Edelman GM, Gall WE, Cowan WM (eds) Molecular bases of neural development. A Neurosciences Institute publication. Wiley, New York, pp 139–160

Rickman M, Amaral DG, Cowan WM (1987) Organization of radial glial cells during the development of the rat dentate gyrus. J Comp Neurol 264:449–479

Sidman RL, Rakic P (1973) Neuronal migration, with special reference to developing human brain: a review. Brain Res 62:1–35

Sotelo C, Bourrat F, Triller A (1984) Postnatal development of the inferior olivary complex in the rat. II. Topographic organization of the immature olivocerebellar projection. J Comp Neurol 222:177–199

Swarz J, Oster-Granite ML (1978) Presence of radial glia in foetal mouse cerebellum. J Neurocytol 7:301–312

Takahashi-Iwanaga H, Kondo H, Yamakuni T, Takahashi Y (1986) An immunohistochemical study on the ontogeny of cells immunoreactive for spot 35 protein, a novel Purkinje cell-specific protein, in the rat cerebellum. Dev Brain Res 29:225–231

Towbin H, Staehelin T, Gordon J (1979) Electrophoretic transfer of proteins from polyacrylamide gels to nitrocellulose sheets: procedure and some applications. Proc Natl Acad Sci USA 76:4350–4354

Voogd J, Bigare F (1980) Topographical distribution of olivary and corticonuclear fibers in the cerebellum: a review. In: Courville J, de Montigny C, Lamarre Y (eds) The inferior olivary nucleus, anatomy and physiology. Raven Press, New York, pp 207–234

Wassef M, Sotelo C (1984) Asynchrony in the expression of guanosine 3′:5′-phosphate-dependent protein kinase by clusters of Purkinje cells during the perinatal development of rat cerebellum. Neuroscience 13:1217–1241

Wassef M, Zanetta JP, Brehier A, Sotelo C (1985) Transient biochemical compartmentalization of Purkinje cells during early cerebellar development. Dev Biol 111:129–137

Wetts R, Herrup K (1982) Cerebellar Purkinje cells are descended from a small number of progenitors committed during early development: quantitative analysis of lurcher chimeric mice. J Neurosci 2:1494–1498

Yamakuni T, Usui H, Iwanaga T, Kondo H, Odani S, Takahashi Y (1984) Isolation and immunohistochemical localization of a cerebellar protein. Neurosci Lett 45:235–240

Yoshida Y, Yamada M, Wakabayashi K, Ikuta F (1987) Immunohistochemical detection of DNA replicating cells in the developing nervous system: use of bromodeoxyuridine and its monoclonal antibody to rat fetuses. Biomed Res 8:431–444